J Biomol NMR (2010) 46:299–305
DOI 10.1007/s10858-010-9402-3

ARTICLE

Precise structural determination of weakly binding peptides by utilizing dihedral angle constraints

Yumiko Mizukoshi · Michiko Nagasu · Ichio Shimada · Hideo Takahashi

Received: 22 October 2009 / Accepted: 24 February 2010 / Published online: 14 March 2010

Abstract Structural determination of target-bound conformations of peptides is of primary importance for the optimization of peptide ligands and peptide–mimetic design. In the structural determination of weakly binding ligands, transferred nuclear Overhauser effect (TrNOE) methods have been widely used. However, not many distance constraints can be obtained from small peptide ligands by TrNOE, especially for peptides bound to a target molecule in an extended conformation. Therefore, for precise structural determination of weakly binding peptides, additional structural constraints are required. Here, we present a strategy to systematically introduce dihedral angle constraints obtained from multiple transferred cross-correlated relaxation experiments and demonstrate precise structures of weakly binding peptides. As a result, we could determine the bioactive conformations of phage-derived peptide ligands and define their core binding motifs.

Keywords Peptide ligand · Weak binding · Structure determination · Cross-correlated relaxation · Dihedral angle

Introduction

Peptide ligands are often used as pharmaceuticals and to study those biological processes that they promote or inhibit (Hruby 2002). With the development of combinatorial approaches such as phage libraries, more and more peptide ligands are being identified and studied (Smith 1985; Scott and Smith 1990; Cwirla et al. 1990; Sidhu et al. 2003).

Structural determination of target-bound conformations of peptides is of primary importance for the optimization of peptide ligands and peptide–mimetic design. In the structural determination of weakly binding ligands, transferred nuclear Overhauser effect (TrNOE) methods have been widely used (Clore and Gronenborn 1982; Ni 1994). However, not many distance constraints can be obtained from small peptide ligands by TrNOE, especially for peptides bound to a target molecule in an extended conformation. Therefore, for precise structural determination of weakly binding peptides, additional structural constraints are required.

More than a decade ago, cross-correlated relaxation (CCR) experiments were proposed for determining the backbone dihedral angle Ψ (Fig. 1a, b; Reif et al. 1997; Yang et al. 1997) and it has been demonstrated that these CCR phenomena can be utilized for structural determination of weakly binding ligands in the so-called transferred CCR (TrCCR) regime as an analogy of TrNOE (Blommers et al. 1999; Carlomagno et al. 1999; Carlomagno et al. 2003). However, thereafter, dihedral angle constraints

Electronic supplementary material The online version of this article (doi:10.1007/s10858-010-9402-3) contains supplementary material, which is available to authorized users.

Y. Mizukoshi · M. Nagasu · I. Shimada · H. Takahashi (✉)
Biomedicinal Information Research Center (BIRC), National Institute of Advanced Industrial Science and Technology (AIST), Aomi 2-41-6, Koto-ku, Tokyo 135-0064, Japan
e-mail: hid.takahashi@aist.go.jp

Y. Mizukoshi · M. Nagasu
Japan Biological Informatics Consortium (JBIC), Aomi 2-41-6, Koto-ku, Tokyo 135-0064, Japan

I. Shimada (✉)
Graduate School of Pharmaceutical Sciences, The University of Tokyo, Hongo 7-3-1, Bunkyo-ku, Tokyo 113-0033, Japan
e-mail: shimada@iw-nmr.f.u-tokyo.ac.jp

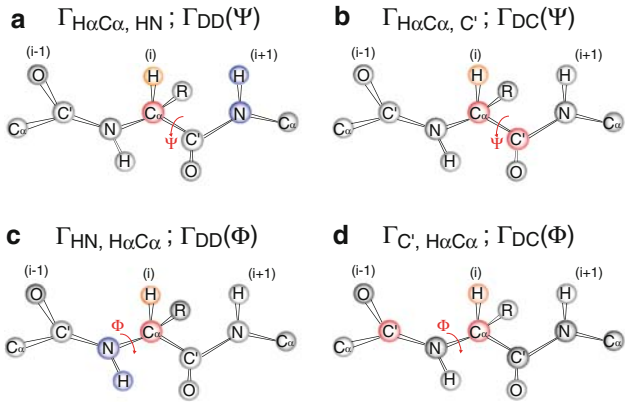

Fig. 1 Schematic representation of four cross-correlated spin relaxation rates associated with determination of backbone dihedral angles Ψ(**a**, **b**) and Φ (**c**, **d**). Here, $\Gamma_{X,Y}$ describes the cross-correlated relaxation rate between X and Y, where X and Y represent dipole–dipole interactions between a proton and a heteronucleus or chemical shift anisotropy (CSA) of a heteronucleus. Each CCR rate is paraphrased with Γ_{DD} or Γ_{DC}, where DD represents the tensor interaction between two dipolar couplings and DC represents the tensor interaction between a dipole coupling and a CSA. Ψ or Φ in parenthesis indicates that the CCR rate is used to obtain information about the corresponding backbone dihedral angle

derived from CCR experiments were not frequently used in structural determination of weakly binding peptides (Blommers et al. 2007). One reason might be that there are some complexities in obtaining information about the backbone dihedral angle Φ (Fig. 1c, d) by utilizing CCR experiments (Pelupessy et al. 1999; Kloiber and Konrat 2000; Kloiber et al. 2002). Recently, we developed a novel and simple two-dimensional version of quantitative CCR experiments for determining Φ angles (Fig. 1c, d; Takahashi and Shimada 2007), and these pairwise CCR experiments enabled us to utilize the dihedral angle constraints of Φ angles with the same criteria as the dihedral angle constraints of Ψ angles.

Here, we present a strategy to systematically introduce dihedral angle constraints obtained from multiple TrCCR experiments and demonstrate precise structures of weakly binding peptides. As a result, we could determine the bioactive conformations of phage-derived peptide ligands and define their core binding motifs.

Materials and methods

NMR sample preparation

Non-labeled peptides were synthesized commercially and purchased from Bex (Tokyo, Japan). Isotope labeled peptides were purified from the cleavable phage library system (Mizukoshi et al. 2006), or KSI-fusion vectors (Novagen, Madison, WI) were constructed and expressed in *E. coli* BLR (DE3) pLys S. Anti-FasL antibody, RNOK2 (Nisihara et al. 2001) was gifted from Chemo-Sero-Therapeutic Research Institute (Kumamoto, Japan). The lyophilized peptides were resuspended in NMR buffer (20 mM phosphate, pH 6.0, 95% H_2O/5% D_2O).

NMR spectroscopy

NMR measurements were recorded on a Bruker Avance 600 equipped with a cryo-cooled triple resonance probe or Bruker Avance 700 spectrometer.

TrNOE

Two-dimensional TrNOE experiments were performed at 313 K on a Bruker Avance 600 equipped with a cryo-cooled triple resonance probe. For the attenuation of broad resonances of large proteins, a relaxation filter that utilizes spin-locking of z-magnetizations after the preparation delay was applied. Spectra of free peptides were acquired on 1.5 mM synthetic peptide and spectra of complexes were acquired on a mix of 1.5 mM synthetic peptide and 90 μM protein. NOE spectra were recorded with 400 complex t_1 points and 1 K complex t_2 points. Optimal conditions for TrNOE measurements were determined by using mixing times of 25, 50, 75, 100, 150, and 200 ms. Since the NOE build up curve showed monotonic increase until mixing time of around 75 ms, and we use the NOE data of mixing times of 50 ms (Supporting Figure S1). In this condition, NOE cross-peaks originating from the peptide in the absence of the target protein were mostly suppressed.

Cross-correlation between ^{15}N-^{1}H dipolar–dipolar interactions and ^{15}N chemical shift anisotropy (DD/CSA)

^{15}N-^{1}H DD/CSA experiments were carried out at 310 K on a sample of 2 mM ^{15}N, ^{13}C-labeled peptide with or without 100 μM protein. The pulse sequence was according to Tjandra et al. (Tjandra et al. 1996). Data matrices acquired at 700 MHz consisted of 1024(t_2) × 80(t_1) data points. A total of 128 scans per complex t_1 increment were collected in 'reference', whereas 512 scans were for 'cross' experiment. The CCR relaxation period was set to 40 ms. Data were processed and analyzed using by NMRPipe (Delaglio et al. 1995).

Cross-correlation experiments for dihedral angles Ψ and Φ

The CCR experiments were applied to 2 mM ^{15}N, ^{13}C-labeled peptides with or without 100 μM protein in NMR

buffer. All spectra were recorded at 310 K. The pulse sequences for measurement of $\Gamma_{H\alpha C\alpha,HN}(\Psi)$ and $\Gamma_{H\alpha C\alpha,C'}(\Psi)$ were intrinsically the same as those published by Chiarparin (Chiarparin et al. 1999). The pulse sequences for measurement of $\Gamma_{HN,H\alpha C\alpha}(\Phi)$ and $\Gamma_{C',H\alpha C\alpha}(\Phi)$ were those established in our laboratory (Takahashi and Shimada 2007). In all CCR experiments, the constant time delay in which cross-correlated relaxation is operative was 28 ms. In the $\Gamma_{H\alpha C\alpha,HN}(\Psi)$ measurements, spectra of free peptide for 'reference' and 'cross' measurements were recorded using 32 and 512 scans, with corresponding acquisition times of 1 and 13 h, respectively. For peptide–protein complexes, spectra for 'reference' and 'cross' measurements were recorded using 64 and 512 scans, with corresponding acquisition times of 2 and 13 h, respectively. In the $\Gamma_{H\alpha C\alpha,C'}(\Psi)$ measurements, spectra of free peptide for 'reference' and 'cross' measurements were recorded using 16 and 256 scans, with corresponding acquisition times of 0.5 and 4.5 h, respectively. For peptide–protein complexes, spectra for reference and cross measurements were recorded using 32 and 512 scans, with corresponding acquisition times of 1 and 13 h, respectively. In the measurement of $\Gamma_{HN,\ H\alpha C\alpha}(\Phi)$, spectra of free peptide for 'reference' and 'cross' measurements were recorded using 64 and 512 transients per FID, with corresponding acquisition times of 1.5 and 14 h, respectively. For peptide–protein complexes, spectra for reference and cross measurements were recorded using 64 and 1024 scans, with corresponding acquisition times of 1.5 and 27 h, respectively. In the measurement of $\Gamma_{C',H\alpha C\alpha}(\Phi)$, spectra of free peptide for 'reference' and 'cross' measurements were recorded using 32 and 512 scans, with corresponding acquisition times of 1 and 14 h, respectively. For peptide–protein complexes, spectra for reference and cross measurements were recorded using 64 and 512 scans, with corresponding acquisition times of 2 and 14 h, respectively. The data were processed and analyzed using NMRPipe (Delaglio et al. 1995). The cross-correlated relaxation rates of both experiments were obtained from the normalized intensity ratios between reference and cross experiments in considering the different number of scans.

Structure calculation

Transferred-NOESY data were used to extract distance restraints for quantitative structure calculations. The cross-peak intensities were calibrated using the cross-peak intensities of the resolved phenyl-ring Hδ-Hε (Phe^3) for P1 or indole-ring Hη2-Hζ2 (Trp^{10}) for P2, correlation peaks assuming an internuclear distance of 2.46 Å. Quantitative distances were obtained according to the literature (Eisenmesser et al. 2000). Dihedral angle constraints from the TrCCR experiments were introduced to the structure calculation, as described in Sect. "Results and discussion". Allowed ranges for the dihedral angle constraints are estimated by the experimental errors of the TrCCR experiments, as well as the possible variety of the residue-specific C′ CSA tensor parameters (Loth et al. 2005, Supporting Figure S2).

CYANA v.2.1 (Herrmann et al. 2002) was used to compute 200 conformers. The 20 lowest target function structures were chosen for the final structure ensemble. The computer programs MOLMOL (Koradi et al. 1996) and PROCHECK-NMR (Laskowski et al. 1996) were used for visualization and analysis of generated peptide structures.

Results and discussion

In this study, we used two individual peptides (P1, SPFARPLLSYGSGD^{homo}S; and P2, LDTPVPRPPWGS GD^{homo}S; Mizukoshi et al. 2006). Their common C-terminal Gly-Ser-Gly-Asp-^{homo}Ser sequence is a 4-residue linker (GSGD) and the reaction product (^{homo}Ser) of the cleavable Met residue by CNBr cleavage. These peptides were obtained from a random peptide library and bound to an anti-Fas-ligand antibody (RNOK2: ~150 kDa; Nisihara et al. 2001). Competitive NMR analyses indicated that both peptides, in spite of the absence of sequence homology, bound to an identical site on the target molecule (Mizukoshi et al. 2006). The dissociation constants of both peptides against RNOK2 are 4×10^{-4} M, and this range of binding affinity is suitable for TrNOE experiments. As a result of the TrNOE experiments, we collected 41 intraresidue and 25 interresidue TrNOE cross-peaks for P1, and 33 intraresidue and 18 interresidue TrNOE cross-peaks for P2. In the case of P1, almost all TrNOE cross-peaks were found in residues 3–8, and in the case of P2, most cross-peaks were found in residues 5–10. These results suggest that the C-terminal linker region does not tightly bind to the antibody molecule. Furthermore, the fact that no cross-peaks between the backbone amide protons and no inter-residual long-range cross-peaks (i–$j > 4$) were observed suggests that these peptides bind to the RNOK2 molecule in an extended conformation. Actually, the structures calculated by using these distance constraints showed the extended forms (Fig. 3a, c). However, these structures were not well converged and the backbone RMSD is 1.47 ± 0.30 Å for P1 and 1.32 ± 0.37 Å for P2. Therefore, we could not obtain precise structural information, such as side chain orientation, from these structures.

For more precise structures, we collected TrCCR data for backbone dihedral angles as follows. First, in order to assess the contact region of the peptides to the target molecule, we measured the cross-correlation between ^{15}N-^{1}H dipole–dipole and ^{15}N chemical shift anisotropy (CSA),

represented as $\Gamma_{HN,N}$, (Tjandra et al. 1996) of these peptides with and without RNOK2. Since the CCR rate depends on the rotational correlation time τ_c, the relaxation property of resonances originating from an excess amount of free ligand is dominated by a small amount of the bound state in weakly binding systems, if the molecular weight of the target receptor molecule is large enough compared with that of the ligand, just as with the TrNOE experiment. Furthermore, this TrCCR would be affected by the local correlation time of the binding ligand, and more specifically, how tightly each part of the ligand molecule binds to the target molecule. As pointed out by Bodenhausen et al. an appropriate exchange rate is required for observing TrCCR phenomena (Ravindranathan et al. 2003). The exchange rate can be controlled to some extent by a choice of experimental conditions (temperature, pH, etc.). Therefore, through these TrCCR ($\Gamma_{HN,N}$) experiments, one can optimize the experimental conditions to enhance the TrCCR phenomena. As a result of these experiments, we could restrict the region for introducing dihedral angle constraints from residues 2 to 10 for both peptides (Supporting Figure S3).

Next, we performed a suite of TrCCR measurements to obtain information about the backbone dihedral angles Ψ and Φ (Fig. 1). The pulse sequences for the measurement of $\Gamma_{DD}(\Psi)$ and $\Gamma_{DC}(\Psi)$ were intrinsically the same as those published by Chiarparin (Chiarparin et al. 1999) and those of $\Gamma_{DD}(\Phi)$ and $\Gamma_{DC}(\Phi)$ were the same as those established in our laboratory (Takahashi and Shimada 2007). In the case of the TrCCR experiments for the weakly binding ligands, the observed CCR rate, Γ^{obs}, is a weighted average between the CCR rate of the free state and that of the bound state, represented as follows:

$$\Gamma^{obs} = (1-\alpha)\Gamma^{free} + \alpha\Gamma^{bound} = \Gamma^{free} + \alpha(\Gamma^{bound} - \Gamma^{free}) \quad (1)$$

where α is the fraction of the bound ligand. If the relaxation in the bound state is dominant, i.e., $\tau_c^{free} << \tau_c^{bound}$; therefore $\Gamma^{free} << \Gamma^{bound}$, and the difference between Γ^{obs} and Γ^{free} is approximated by $\alpha\Gamma^{bound}$. Therefore, the CCR rates in the bound states multiplied by the fraction of the bound state can be described as follows:

$$\alpha\Gamma^{bound} = \Gamma^{obs} - \Gamma^{free} \quad (2)$$

In order to obtain Γ^{free} and Γ^{obs}, ^{13}C, ^{15}N-labeled peptides were subjected to two sets of pairwise CCR experiments mentioned above with or without RNOK2, respectively. Lists of obtained CCR rates ($\alpha\Gamma_{DD}^{bound}(\Psi)$, $\alpha\Gamma_{DC}^{bound}(\Psi)$; $\alpha\Gamma_{DD}^{bound}(\Phi)$, and $\alpha\Gamma_{DC}^{bound}(\Phi)$) are shown as $\alpha\Gamma_{DD}$ and $\alpha\Gamma_{DC}$ in Table 1 and Supporting Table S1

Table 1 CCR rate of P1, $\alpha\Gamma_{DD}$, $\alpha\Gamma_{DC}$, Γ_{DC}/Γ_{DD} and dihedral angle constraints (Ψ: upper panel, Φ: lower panel)

Residue	$\alpha\Gamma_{DD}$ (s^{-1})	$\alpha\Gamma_{DC}$ (s^{-1})	Γ_{DC}/Γ_{DD}	Angle constraints (Ψ)
Pro2	−2.47 ± 0.21	−0.04 ± 0.05	0.016 ± 0.020	100° ± 10° or 140° ± 10°
Phe3	−1.95 ± 0.23	−0.57 ± 0.05	0.292 ± 0.043	90° ± 10° or 150° ± 10°
Ala4	−1.98 ± 0.13	0.97 ± 0.03	−0.490 ± 0.036	120° ± 20°
Arg5	ND	ND		
Pro6	−2.30 ± 0.10	−0.76 ± 0.03	0.330 ± 0.019	90° ± 10° or 150° ± 10°
Leu7	−1.94 ± 0.08	0.25 ± 0.03	−0.129 ± 0.016	120° ± 20°
Leu8	−1.37 ± 0.35	0.64 ± 0.07	−0.467 ± 0.130	120° ± 20°
Ser9	−0.50 ± 0.15	−0.26 ± 0.04	0.520 ± 0.175	90° ± 10° or 150° ± 10°
Tyr10	−0.36 ± 0.19	−0.36 ± 0.04	1.000 ± 0.539	80° ± 10° or 160° ± 10°
Residue	$\alpha\Gamma_{DD}$ (s^{-1})	$\alpha\Gamma_{DC}$ (s^{-1})	Γ_{DC}/Γ_{DD}	Angle constraints (Φ)
Pro2	ND	ND		
Phe3	−2.70 ± 0.35	0.18 ± 0.13[a]	−0.067 ± 0.049	−120° ± 20°
Ala4	−2.17 ± 0.36	−1.06 ± 0.14	0.488 ± 0.104	−150° ± 10° or −90° ± 10°
Arg5	−2.08 ± 0.22	−0.33 ± 0.11	0.159 ± 0.055	−150° ± 10° or −90° ± 10°
Pro6	ND	ND		
Leu7	−1.24 ± 0.15	−0.95 ± 0.09	0.760 ± 0.118	−160° ± 10° or −80° ± 10°
Leu8	−0.75 ± 0.10	−1.45 ± 0.07	1.932 ± 0.274	−160° ± 10° or −80° ± 10°
Ser9	−2.15 ± 0.45	−0.38 ± 0.19	0.176 ± 0.096	−150° ± 10° or −90° ± 10°
Tyr10	−1.57 ± 0.21	−0.33 ± 0.09	0.210 ± 0.064	−150° ± 10° or −90° ± 10°

Error estimations were performed according to the literature (Carlomagno and Griesinger 2000). ND means no signal to be detected. [a]The signal intensities in cross experiments showed undetectable small values, and the intensities were set to zero ± standard deviation of noise intensities in CCR rate calculations

For the following step, the dihedral angle constraints can be obtained from these CCR rates as described below. First, by comparing the signs and the relative intensities of the pairwise CCR rates ($\alpha\Gamma_{DD}$ and $\alpha\Gamma_{DC}$) with their theoretical curves (Fig. 2a or b), we can restrict appropriate angular regions for both the dihedral angles Ψ and Φ. For the dihedral angle Ψ, when $\Gamma_{DD}(\Psi)$ shows a positive value and $\Gamma_{DC}(\Psi)$ shows a negative or small positive value, the appropriate angular regions should be limited between -180 and $-85°$ or -35 and 60°. In the case of a negative value for $\Gamma_{DD}(\Psi)$, if $\Gamma_{DC}(\Psi)$ shows a relatively large positive, the appropriate regions should be limited between -85 and $-35°$; on the other hand, if $\Gamma_{DC}(\Psi)$ shows a negative or small positive value, the appropriate regions should be limited between 60 and 180°. In the similar manner, the appropriate regions for the dihedral angle Φ could be approximately defined in the first step. Next, in order to tightly define the range, we calculate the $\alpha\Gamma_{DC}/\alpha\Gamma_{DD} = \Gamma_{DC}/\Gamma_{DD}$ values (Blommers et al. 1999; Carlomagno et al. 2003). This calculated value in principle removes the common terms between Γ_{DD} and Γ_{DC}, and therefore alleviates the issues concerning small ligands which weakly bind to the large target molecules, like overall τ_c and its anisotropy in the bound state, and the population of the bound state.

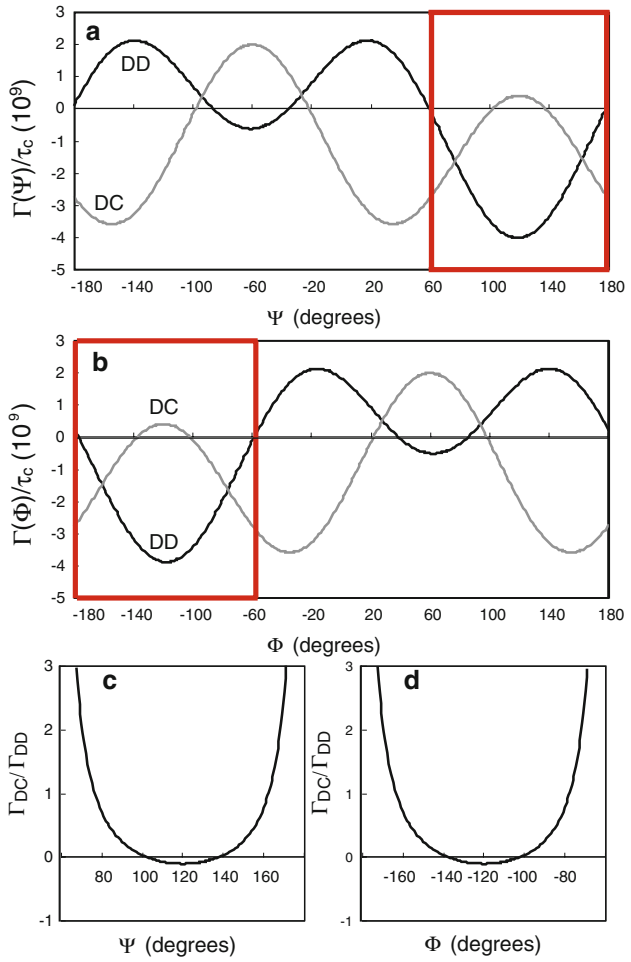

Fig. 2 Theoretical curves of Ψ (**a**) & Φ (**b**) angles as a function of the peptide backbone dihedral angles (Schwalbe et al. 2001). Theoretical curves of Γ_{DC}/Γ_{DD} values for dihedral angles Ψ (**c**) and Φ (**d**). Standard bond lengths and angles ($\gamma_{NH} = 1.02$ Å and $\gamma_{CH} = 1.09$ Å) were used for the calculation. CSA tensor parameters of C' nuclei values σ_{xx}, σ_{yy} and σ_{zz} were assumed to be 244, 178, and 90 ppm, respectively (Teng et al. 1992)

In this study, by first comparing the pairwise CCR rates, $\Gamma_{DD}(\Psi)$ showed negative values and $\Gamma_{DC}(\Psi)$ showed negative or small positive values. Therefore, the appropriate regions should be limited between 60 and 180°, as shown in the red frames in Fig. 2a. In the same way, the appropriate regions for dihedral angle Φ were limited between -180 and $-60°$, as shown in the red frames in Fig. 2b. Next, we calculated Γ_{DC}/Γ_{DD} values and, consequently, more tightly defined constraints for dihedral angles Ψ and Φ could be obtained. The criterion was set as follows. If the Γ_{DC}/Γ_{DD} value for Ψ is negative, the dihedral angle Ψ is constrained between 100 and 140°. If the value is positive and less than 0.1, the dihedral angle constraints for Ψ are set to $100 \pm 10°$ or $140 \pm 10°$. If the value is between 0.1 and 0.6, the constraints for Ψ are set to $90 \pm 10°$ or $150 \pm 10°$. If the value is more than 0.6, the constraints are $80 \pm 10°$ or $160 \pm 10°$. Taking into consideration the cumulated uncertainties for the measurements (Vögeli and Yao 2009) and intrinsic diversity of residue-specific CSA (Markwick and Sattler 2004; Loth et al. 2005), the uncertainty of the dihedral angle constraints are set to $\pm 10°$. To obtain more accurate CCR rates avoiding systematic errors, one should carry out experiments, using multiple constant time delays (Chiarparin et al. 1999).

In the case of the dihedral angle Φ, the same procedure should be followed (Fig. 2b, d). The dihedral constraints for Ψ and Φ angles of both P1 and P2 were obtained and are summarized in Table 1 and Supporting Table S1, respectively. A total of 15 angle constraints were systematically obtained for P1 and 8 angle constraints were obtained for P2. In addition to these angle constraints obtained from TrNOE experiments, peptide conformations were calculated. Out of the 200 generated structures, 20 structures with the lowest target function were selected, and no structure had NOE violations greater than 0.2 Å for either P1 or P2. The structural statistics are shown in supporting information (Supporting Tables S2 and S3). As shown in Fig. 3, 20 selected structures were well converged compared with those from the distance constraints alone. The backbone RMSD value was improved from 1.47 ± 0.30 Å to 0.94 ± 0.27 Å for P1 and from 1.32 ± 0.37 Å to 0.37 ± 0.10 Å for P2.

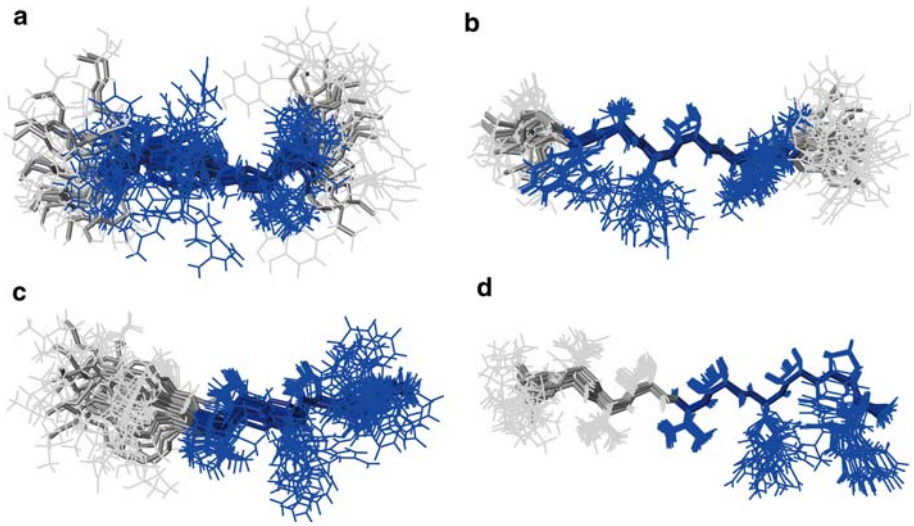

Fig. 3 The 20 converged structures of P1 (**a**, **b**) and P2 (**c**, **d**) bound to RNOK2 obtained from TrNOE experiments alone (**a**, **c**) and TrNOE experiments with TrCCR experiments (**b**, **d**). Structures were fitted to backbone aroms. The *blue regions* are fitted regions; residues 3–8 for P1, and residues 5–10 for P2. The *thick lines* represent backbone atoms

On the other hand, the essential residues for binding were identified to be Phe^3, Arg^5, and Leu^8 of P1 and Val^5, Arg^7, and Trp^{10} of P2 by alanine-substitution (Supporting Table S4). According to the peptide structures of the lowest target function, which we determined by utilizing TrCCR data, the backbones of two individual peptides were superimposed with a small RMSD value of 1.06 Å and the side chains of the important residues were oriented in a similar direction (Fig. 4). Nishimura et al. investigated the epitope of FasL against RNOK2 antibody by the mutational studies, which revealed that the contact region is quite large, and some discontinuous residues including Arg^{198} were critical for the binding (Nisihara et al. 2001). Both peptides assumed the extended conformation in the bound state and include Arg residue (Arg^5 of P1 and Arg^7 of P2), which might mimic a local part of the epitope. These results suggest that the precise determination of the bound conformation of the ligand provides a more concrete view of the structure-function relationship for the active ligand molecule.

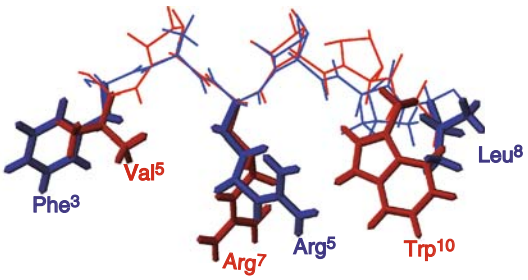

Fig. 4 Overlay of P1 (*blue*) with P2 (*red*). The lowest energy structure for each peptide is superimposed over the backbone atoms of residues (Phe^3-Leu^8 for P1 and Val^5-Trp^{10} for P2) that are critical for binding to the target molecule. The *thick lines* represent sidechains of important residues from alanine-substitution experiments

In this study, we did not obtain any evidence of multiple conformations from our NMR data. In particular, we obtain two different kinds of structural parameters—that is, distance constraints and dihedral angles constraints, based on TrNOE experiments and TrCCR experiments, respectively, and there is no conflict between these data. If each data is conflict, one should consider the possibility of multiple conformations in the bound state. In other words, these complementary experiments would also be useful for the validation of determined structure.

In conclusion, we determined the precise structures of weakly binding peptides by comprehensively introducing dihedral angle constraints from a suite of CCR experiments. The fact that the precise tertiary structures of the peptide ligands in the bound state can be obtained easily in this way accelerates the study of rational design of peptides and/or small molecules with higher affinity to target molecules.

Acknowledgments We thank the Chemo-Sero-Therapeutic Research Institute for providing the anti-FasL antibody, RNOK2. This work was supported by grants from New Energy and Industrial Technology Development Organization.

References

Blommers MJJ, Stark W, Jones CE, Head D, Owen CE, Jahnke W (1999) Transferred cross-correlated relaxation complements transferred NOE: structure of an IL-4R-derived peptide bound to STAT-6. J Am Chem Soc 121:1949–1953

Blommers MJJ, Strauss A, Geiser M, Ramage P, Sparrer H, Jahnke W (2007) NMR-based strategies to elucidate bioactive conformations of weakly binding ligands. Top Curr Chem 128:16

Carlomagno T, Griesinger C (2000) Errors in the measurement of cross-correlated relaxation rates and how to avoid them. J Magn Reson 144:280–287

Carlomagno T, Felli IC, Czech M, Fischer R, Sprinzl M, Griesinger C (1999) Transferred cross-correlated relaxation: application to

the determination of sugar pucker in an aminoacylated tRNA-mimetic weakly bound to EF-Tu. J Am Chem Soc 121: 1945–1948

Carlomagno T, Sánchez VM, Blommers MJJ, Griesinger C (2003) Derivation of dihedral angles from CH-CH dipolar-dipolar cross-correlated relaxation rates: a C-C torsion involving a quaternary carbon atom in epothilone A bound to tubulin. Angew Chem Int Ed 42:2515–2517

Chiarparin E, Pelupessy P, Ghose R, Bodenhausen G (1999) Relaxation of two-spin coherence due to cross-correlated fluctuations of dipole-dipole couplings and anisotropic shifts in NMR of ^{15}N, ^{13}C-labeled biomolecules. J Am Chem Soc 121:6876–6883

Clore GM, Gronenborn AM (1982) Theory and applications of the transferred nuclear Overhauser effect to the study of conformations of small ligands bound to proteins. J Magn Res 48:402–417

Cwirla SE, Peters EA, Barrett RW, Dower WJ (1990) Peptides on phage: a vast library of peptides for identifying ligands. Proc Acad Sci Natl USA 87:6378–6382

Delaglio F, Grzesiek S, Vuister GW, Zhu G, Pfeifer J, Bax A (1995) NMRPipe: a multidimensional spectral processing system based on UNIX pipes. J Biomol NMR 6:277–293

Eisenmesser EZ, Zabell APR, Post CB (2000) Accuracy of bound peptide structures determined by exchange transferred nuclear Overhauser data: a simulation study. J Biomol NMR 17:17–32

Herrmann T, Güntert P, Wüthrich K (2002) Protein NMR structure determination with automated NOE assignment using the new software CANDID and torsion angle dynamics algorithm DYANA. J Mol Biol 319:209–227

Hruby VJ (2002) Designing peptide receptor agonists and antagonists. Nat Rev Drug Discov 1:847–858

Kloiber K, Konrat R (2000) Measurement of the protein backbone dihedral angle φ based on quantification of remote CSA/DD interference in inter-residue ^{13}C'(i - 1)-^{13}C$_\alpha$(i) multiple-quantum coherences. J Biomol NMR 17:265–268

Kloiber K, Schüler W, Konrat R (2002) Automated NMR determination of protein backbone dihedral angles from cross-correlated spin relaxation. J Biomol NMR 22:349–363

Koradi R, Billeter M, Wüthrich K (1996) MOLMOL: a program for display and analysis of macromolecular structures. J Mol Graph 14(51–5):29–32

Laskowski RA, Rullmann JAC, MacArthur MW, Kaptein R, Thornton JM (1996) AQUA and PROCHECK-NMR: programs for checking the quality of protein structures solved by NMR. J Biomol NMR 8:477–486

Loth K, Pelupessy P, Bodenhausen G (2005) Chemical shift anisotropy tensors of carbonyl, nitrogen, and amide protein nuclei in proteins through cross-correlated relaxation in NMR spectroscopy. J Am Chem Soc 127:6062–6068

Markwick PRL, Sattler M (2004) Site-specific variations of carbonyl chemical shift anisotropies in proteins. J Am Chem Soc 126: 11424–11425

Mizukoshi Y, Takahashi H, Shimada I (2006) Rapid preparation of stable isotope labeled peptides that bind to target proteins by a phage library system. J Biomol NMR 34:23–30

Ni F (1994) Recent developments in transferred NOE methods. Prog NMR Spectrosc 26:517–606

Nisihara T, Ushio Y, Higuchi H, Kayagaki N, Yamaguchi N, Soejima K, Matsuo S, Maeda H, Eda Y, Okumura K, Yagita H (2001) Humanization and epitope mapping of neutralizing anti-human Fas ligand monoclonal antibodies: structural insights into Fas/Fas ligand interaction. J Immunol 167:3266–3275

Pelupessy P, Chiarparin E, Ghose R, Bodenhausen G (1999) Simultaneous determination of Ψ and Φ angles in proteins from measurements of cross-correlated relaxation effects. J Biomol NMR 14:277–280

Ravindranathan S, Mallet JM, Sinay P, Bodenhausen G (2003) Transferred cross-relaxation and cross-correlation in NMR: effects of intermediate exchange on the determination of the conformation of bound ligands. J Magn Reson 163:199–207

Reif B, Hennig M, Griesinger C (1997) Direct measurement of angles between bond vectors in high-resolution NMR. Science 276: 1230–1233

Schwalbe H, Carlomagno T, Hennig M, Junker J, Reif B, Richter C, Griesinger C (2001) Cross-correlated relaxation for measurement of angles between tensorial interactions. Methods Enzymol 338:35–81

Scott JK, Smith GP (1990) Searching for peptide ligands with an epitope library. Science 249:386–390

Sidhu SS, Fairbrother WJ, Deshayes K (2003) Exploring protein-protein interactions with phage display. ChemBioChem 4:14–25

Smith GP (1985) Filamentous fusion phage: novel expression vectors that display cloned antigens on the virion surface. Science 228:1315–1317

Takahashi H, Shimada I (2007) Pairwise NMR experiments for the determination of protein backbone dihedral angle Φ based on cross-correlated spin relaxation. J Biomol NMR 37:179–185

Teng Q, Iqbal M, Cross TA (1992) Determination of the ^{13}C chemical shift and ^{14}N electric field gradient tensor orientations with respect to the molecular frame in a polypeptide. J Am Chem Soc 114:5312–5321

Tjandra N, Szabo A, Bax A (1996) Protein backbone dynamics and ^{15}N chemical shift anisotropy from quantitative measurement of relaxation interference effects. J Am Chem Soc 118:6986–6991

Vögeli B, Yao L (2009) Correlated dynamics between protein HN and HC bonds observed by NMR cross relaxation. J Am Chem Soc 131:3668–3678

Yang DW, Konrat R, Key LE (1997) A multidimensional NMR experiment for measurement of the protein dihedral angle Ψ; based on cross-correlated relaxation between ^{1}H$_\alpha$-^{13}C$_\alpha$ dipolar and ^{13}C' (carbonyl) chemical shift anisotropy mechanisms. J Am Chem Soc 119:11938–11940